
**Separation Science and Technology**
Publication details, including instructions for authors and subscription information:
http://www.informaworld.com/smpp/title~content=t713708471

# Improvement of the Ultrafiltration of Highly Viscous Liquids by Injection of Pressurized Carbon Dioxide

D. Gourgouillon[a]; L. Schrive[b]; S. Sarrade[b]; G. M. Rios[c]
[a] INSTITUTO DE TECNOLOGIA QUÍMICA E BIOLÓGICA, OEIRAS, PORTUGAL [b] LABORATOIRE DES FLUIDES SUPERCRITIQUES ET DES MEMBRANES, PIERRELATTE, CEDEX, FRANCE [c] LABORATOIRE DES MATÉRIAUX ET DES PROCÉDÉS MEMBRANAIRES UMR 5635, MONTPELLIER, CEDEX, FRANCE

Online publication date: 10 September 2000

**To cite this Article** Gourgouillon, D. , Schrive, L. , Sarrade, S. and Rios, G. M.(2000) 'Improvement of the Ultrafiltration of Highly Viscous Liquids by Injection of Pressurized Carbon Dioxide', Separation Science and Technology, 35: 13, 2045 — 2061
**To link to this Article: DOI:** 10.1081/SS-100102088
**URL:** http://dx.doi.org/10.1081/SS-100102088

SEPARATION SCIENCE AND TECHNOLOGY, **35**(13), pp. 2045–2061, 2000

# Improvement of the Ultrafiltration of Highly Viscous Liquids by Injection of Pressurized Carbon Dioxide

D. GOURGOUILLON*
INSTITUTO DE TECNOLOGIA QUÍMICA E BIOLÓGICA
AV. DA REPUBLICA, QUINTA DO MARQUES, APARTADO 127
2780-901 OEIRAS, PORTUGAL

L. SCHRIVE and S. SARRADE
COMMISSARIAT À L'ÉNERGIE ATOMIQUE, DCC/DTE/SLC
LABORATOIRE DES FLUIDES SUPERCRITIQUES ET DES MEMBRANES
BP 111, 26702 PIERRELATTE CEDEX, FRANCE

G. M. RIOS
LABORATOIRE DES MATÉRIAUX ET DES PROCÉDÉS MEMBRANAIRES UMR 5635
ECOLE NATIONALE SUPÉRIEURE DE CHIMIE, 276 RUE DE LA GALÉRA
34097 MONTPELLIER CEDEX, FRANCE



## ABSTRACT

The injection of pressurized carbon dioxide ($CO_2$) (gas or supercritical) in a liquid induces a lowering of viscosity the magnitude of which is a function of temperature and pressure. In this work, the addition of pressurized $CO_2$ to highly viscous liquids is proposed as an ecologically viable and economically competitive technology to increase permeate flux during ultrafiltration at low temperature. Initially viscosity and phase-equilibrium data of model compounds, polyethylene glycols (PEG), in the presence of $CO_2$ were studied at high pressure. Then tangential filtration runs with PEG-$CO_2$ mixtures were conducted on pilot-plant units equipped with mineral membranes. Results thus obtained were analyzed using the previously measured kinetic and thermodynamic data.

*Key Words.* Ultrafiltration; Polyethylene glycol; Carbon dioxide; Viscosity; Phase equilibria

*To whom correspondence should be addressed.

## INTRODUCTION

Low energy consumption, ease of use, safety, or environmental compatibility are many arguments that explain the growing interest for membrane processes in the industry. Ultrafiltration (UF) is a technique mainly used for liquid waste treatment, concentration of biological solutions, and, more generally, fractionation of mixtures involving at least one macromolecular species (e.g., proteins). The membrane rejects macromolecular species, whereas smaller compounds are allowed to go through it. Ceramic asymmetric membranes, consisting of thin selective mesoporous skin deposited on a thicker support that gives the unit its mechanical resistance, exhibit many advantages compared to traditional organic elements: high resistance to chemicals, thermal and mechanical degradation, long lifetime, and easy cleaning, even with extreme pH solutions. The use of tubular modules allows working with high tangential velocities and shear stresses, thus making it possible to reduce limitations resulting from polarization and fouling phenomena.



The regeneration and valorization by filtration of products such as oils have seldom been implemented because these fluids are highly viscous and difficult to handle at ambient temperature. Indeed, the performance of traditional tangential filtration processes of micro-, ultra-, and nanofiltration are strongly dependent on product viscosity, as indicated by the Darcy equation: high viscosities lead to low transmembrane fluxes and high energy expenditure. However, the intrinsic characteristics of membrane processes make them attractive for used-oil regeneration, in that they could advantageously replace the traditional and polluting processes of incineration or regeneration by acid/clay treatment. Moreover, a recent study shows that oil recycling is more profitable from an energy point of view than incineration (1).

A means of overcoming the difficulty previously mentioned is to operate at high temperatures (2–4), which involves a lowering of viscosity. However, even for relatively high temperatures (200–300°C), the oil viscosity remains much higher than that of aqueous solutions, and permeate fluxes are too low for industrial applications. Another alternative consists of diluting the viscous fluid with an appropriate liquid solvent (5–7), but this technology is not economically viable because of the need for further expensive separation stages (e.g., distillation, centrifugation).

Under pressure and temperature conditions above the critical point ($P > P_c$ and $T > T_c$), a pure substance is called a supercritical fluid (SCF). SCFs often constitute a convenient alternative to the use of conventional or chlorinated solvents (8) for the manufacture of high-added-value products (9), for applications where the environmental constraints are particularly important, or sometimes when coupled processes such as extraction and filtration can be developed (10). Indeed, in an easily accessible range of pressure for industrial

processes ($P < 50$ MPa), SCFs offer numerous advantages of both gases and liquids:

- a reasonable solvent power resulting from density values close to those of liquids,
- high binary diffusion coefficient values close to those of gases,
- low viscosity values improving mass transfer,
- low surface-tension values for liquid mixtures containing high concentrations of SCF that allow an easy penetration of porous media.

This unusual combination of physicochemical properties can advantageously be exploited in industrial operations for extraction, synthesis, and separation (11). Moreover, it is quite easy to modify these parameters, mainly density and thus solvent strength, continuously, by adjusting the pressure and temperature. That is why they are often called "tunable" solvents.

As previously shown in the literature, the dissolution of $CO_2$ in highly viscous fluids such as melted polymers or oils involves a viscosity reduction (12, 13) that makes it possible to process at lower temperatures. All these facts underline the potential of supercritical $CO_2$ as a means to facilitate UF of used oils at ambient temperature, in an ecologically viable and economically competitive regeneration process (14). Such a process would not require any additional separation step because $CO_2$ could be easily eliminated from the collected fractions by simple decompression.

This paper presents preliminary experiments carried out to validate this concept, with model compounds (PEG) and two different pilot-plant units. The application of the process to real products (mineral and used oils) is in progress and will be the subject of a future publication.



## MATERIALS AND METHODS

Descriptions of the techniques involved to obtain viscosity and thermodynamic data have been recently published (13, 15, 16). Only the methods and apparatuses involved in the filtration of PEG assisted by adding $CO_2$ are presented here.

### Products

The characteristics of the different PEGs used as model compounds are indicated in Table 1.

### Analytical Methods

Pressure-composition phase diagrams for PEG-$CO_2$ systems were obtained by analyzing samples collected from a static view-cell (15). The selectivities

TABLE 1
Characteristics of the PEG

| PEG | Company | Range of fusion/K | Application |
|---|---|---|---|
| 200 | Sigma | 235–237 | Phase equilibria<br>Viscosity PEG-$CO_2$ |
| 400 | Aldrich | 274–279 | Phase equilibria<br>Viscosity PEG-$CO_2$<br>Filtration |
| 600 | Aldrich | 290–296 | Phase equilibria |
| 1000 | Aldrich | 306–313 | Filtration |

of the membranes were calculated by analyzing permeate samples collected during the filtration of a PEG 400-PEG 1000 mixture saturated with pressurized $CO_2$.

All concentration measurements were conducted with a Gel Permeation Chromatograph (Waters). This system is composed of a pump (Model 510), an injector (U6K), a differential refractometer (R401) heated with a thermal-regulated bath (Haake, D1), a thermostated chamber (TCM) in which the column is placed, and an integrator (745 DATED MODULE). The column is an Ultrahydrogel 120 model, well adapted to a range of molar mass ranging from 100 $g \cdot mol^{-1}$ to 5000 $g \cdot mol^{-1}$.



## Pilot-plant Units and Membranes

Two types of pilot-plant units have been successively used in this study:

- a coupling bench, initially devoted to the study of a "nanofiltration plus supercritical fluid extraction" process (10). This bench has been modified to carry out a first series of experiments intended to evaluate the performances of the new process in terms of flux and selectivity.
- a new bench, the so-called FILEAS bench (*FIL*tration *E*xpérimentale *A*ssistée par fluide *S*upercritique), specifically built for this study to acquire reliable data on a wide range of flow regimes and for larger product quantities.

The FILEAS bench is characterized by:

- flow rates inside the module from 0.5 to 3.0 $m^3 \cdot hr^{-1}$ (pump PMH, TF40MP) that make it possible to test the performances of industrial multichannel membranes.
- a sophisticated piece of equipment that allows the recording of operating parameters as a function of time, such as temperature, pressure (Fisher-Rosemount, 3051CD), liquid flow rate (Fisher-Rosemount, DH 006S and

DH100S), gas flow rate (Brooks, 5680 and 5681), viscosity (Sofraser, 6001), and density (Fisher-Rosemount, DH 100S).

- the ability to conduct fully continuous and automated runs over several days.

The bench is presented in Fig. 1. In the loading zone, two pumps allow the introduction of liquid $CO_2$ and liquid polymer (Lewa, FK2) at the required pressure; then mixing and preheating are carried out just before entering the autoclave. The mixture thus obtained (PEG saturated with supercritical $CO_2$) is circulated through the membrane module. Because of the transmembrane pressure, splitting of the solution into two phases takes place. The light compounds-rich phase is called the permeate; the heavy compounds-rich phase is called the retentate. In the separation zone, an isothermal pressure release of each phase takes place. This leads, for both phases, to liquid (concentrate or filtrate) and gas streams at the exits of cyclone separators. The $CO_2$ in the gas state can be recycled at the end of the process.

Two kinds of ceramic membranes have been used (Table 2):

- medium-pore-size UF membranes (cut-off: 50 kDa) for flux measurements. Experiments were conducted with PEG 400 solutions on both coupling and FILEAS benches (membranes T50A, T50B, and T50C). These membranes were provided by TAMI Industries. They are multichannel el-



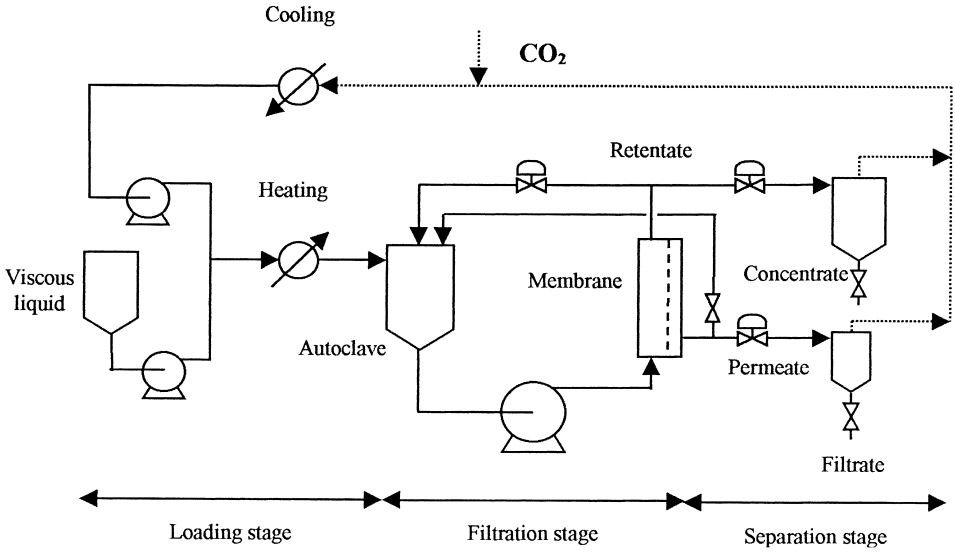


FIG. 1 Schematic of the FILEAS bench.

TABLE 2
Characteristics of the Membranes Used in the Pilot-Plant Units

| Membrane | T50A | T50B | T50C | T511 | T513 |
|---|---|---|---|---|---|
| Company | TAMI | TAMI | TAMI | TAMI | SCT |
| Support | ATZ | ATZ | ATZ | ATZ | $Al_2O_3\alpha$ |
| Layer | $ZrO_2$ | $ZrO_2$ | $ZrO_2$ | $TiO_2^*$ | $TiO_2^*$ |
| Channels | 3 | 3 | 3 | 3 | 1 |
| Cut-off (kDa) | 50 | 50 | 50 | 2 | 2 |
| Length (m) | $25\ 10^{-2}$ | $25\ 10^{-2}$ | $15.5\ 10^{-2}$ | $15.5\ 10^{-2}$ | $15.5\ 10^{-2}$ |
| Total hydraulic diameter (m)† | $10.8\ 10^{-3}$ | $10.8\ 10^{-3}$ | $10.8\ 10^{-3}$ | $10.8\ 10^{-3}$ | $7\ 10^{-3}$ |
| Surface of filtration ($m^2$) | $7.69\ 10^{-3}$ | $7.93\ 10^{-3}$ | $4.71\ 10^{-3}$ | $4.84\ 10^{-3}$ | $2.77\ 10^{-3}$ |
| Cross-section ($m^2$) | $3.3\ 10^{-5}$ | $3.3\ 10^{-5}$ | $3.3\ 10^{-5}$ | $3.3\ 10^{-5}$ | $3.85\ 10^{-5}$ |
| Application | PEG 400 FILEAS | PEG 400 FILEAS | PEG 400 on coupling bench | PEG 400/1000 on coupling bench | PEG 400/1000 on coupling bench |

* Layers deposited by the CEA (Commissariat à l'Energie Atomique).
† Data from TAMI Industries.



ements ("clover" geometry) made of a thin $ZrO_2$ filtering layer deposited on a macroporous support made of $Al_2O_3/TiO_2/ZrO_2$;

- low-pore-size UF membrane (cut-off: 2 kDa), mainly used for selectivity measurements on the coupling bench. These membranes were prepared at CEA (Commissariat à l'Energie Atomique) by sol-gel deposition of a $TiO_2$ thin layer on either a multichannel (from TAMI Industries: T511) or a tubular (from SCT company: T513) support.

Before starting $CO_2$-assisted filtration runs, membranes were characterized as to permeability, rejection, and selectivity with aqueous solutions. Some results are given in Table 3. After each test, washing with NaOH (0.1 N), HCl (0.1 N), and pure water carried out a complete regeneration.

TABLE 3
Permeability, Retention, and Selectivity of the Low Pore Size Membranes T511 and T513 Used on the Coupling Bench

| | Permeability ($l \cdot hr^{-1} \cdot m^{-2} \cdot bar^{-1}$) | | Retention PEG ($5\ g \cdot l^{-1}$)* | | | Selectivity PEG |
|---|---|---|---|---|---|---|
| Membrane | Water | PEG ($15\ g \cdot l^{-1}$) | PEG 200 | PEG 600 | PEG 1500 | 400/1000 |
| T511 | 250 | 180 | 10% | 32% | 68% | 1.5 |
| T513 | 160 | 130 | 12% | 39% | 73% | 1.6 |

* Measurements realized with a solution containing the three PEGs ($5\ g \cdot l^{-1}$ each)

## EXPERIMENTAL RESULTS AND DISCUSSION

### Viscosimetric and Thermodynamic Data

Brief results obtained with PEG 200, PEG 400, and PEG 600 for pressures from 0 MPa to 25 MPa and temperatures from 313 K to 348 K (13) are given here. The viscosity reduction (or "plasticization") associated with the dissolution of a SCF frequently exceeds the reduction obtained with traditional organic solvents. When an organic solvent is used, the lowering of viscosity is due to the effect of dilution of the polymeric chains. When a SCF is used as a viscosity reducing agent or "plasticizer," an additional free volume is generated because of the low density of SCF compared to that of polymers. This phenomenon involves an increased mobility of the chains and consequently a lower viscosity.

The addition of pressurized $CO_2$ induced an exponential decay of the viscosity of PEG (13). However, when the temperature increases or when the molecular mass of the polymer (i.e., its size) decreases, the lowering of viscosity becomes less significant. The highest viscosity reduction was obtained with PEG 400: 89% at 25 MPa and 313 K, corresponding to a mixture whose viscosity is approximately equal to 5 mPa·s and that roughly contains 30% $CO_2$ (by mass). The measured viscosities in temperatures from 313 K to 348 K for the $CO_2$-saturated PEG 400 are plotted in Fig. 2 (13).

Using a static view-cell specifically designed to study phase equilibria for pressurized PEG-$CO_2$ mixtures, pressure—composition curves were obtained



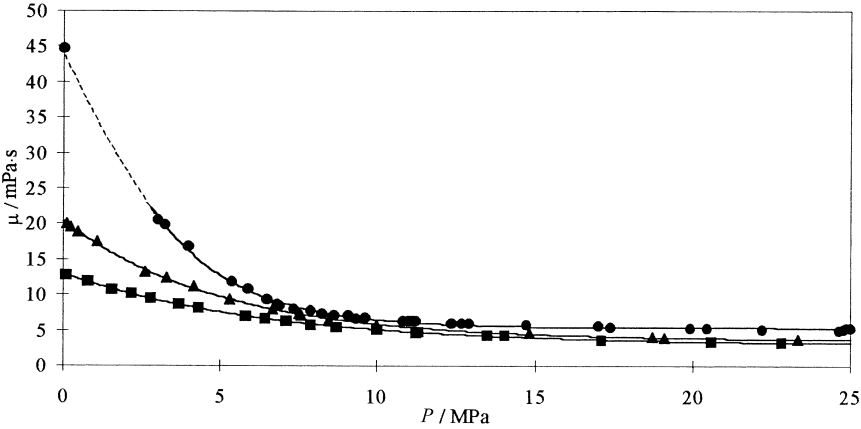


FIG. 2 Plot of $CO_2$-saturated PEG 400 viscosity vs. $CO_2$ pressure at 313 K (●), 333 K (▲), and 348 (■) (13).

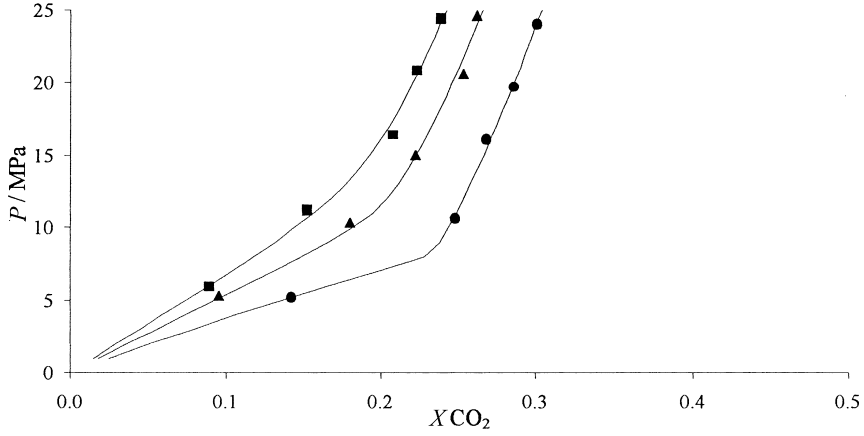


FIG. 3 Phase diagram ($P$, $X$) for the system PEG 400-$CO_2$ at 313 K (●), 333 K (▲), and 348 K (■). $P$ represents the pressure, and $X$ is the $CO_2$ mass fraction in the polymer-rich fluid. The solid curves represent calculated binodals obtained with the SL EOS (19).



(15, 16). They exhibit the following trend for the three PEG-$CO_2$ systems:

- at constant temperature, the respective solubilities increase with pressure,
- at constant pressure, the respective solubilities decrease when temperature is increased.

Moreover, the solubility of $CO_2$ was essentially molar-mass independent, except in the case of PEG 200, where the influence of the hydroxyl end-groups was significant.

Data points were modeled with the help of the so-called Sanchez-Lacombe Equation of State (SL EOS) (17), which is based on the lattice-fluid theory

$$\tilde{\rho}^2 + \tilde{P} + \tilde{T}\left[\ln(1-\tilde{\rho}) + \left(1 - \frac{1}{r}\right)\tilde{\rho}\right] = 0 \qquad (1)$$

where $\tilde{T}$, $\tilde{P}$, and $\tilde{\rho}$ are the reduced temperature, pressure, and density of the homogeneous phase (one-fluid phase or multicomponent-fluid phase). Experimental data and calculated values for the system $CO_2$-PEG 400, for temperatures from 313 K to 348 K, are plotted in Fig. 3 (15).

## Ultrafiltration Experiments on Pilot-plant Units

### *Coupling bench*

The entire set of experiments was conducted in laminar regime ($Q_m \approx 100$ kg·h$^{-1}$, $u \approx 0.7$ m·s$^{-1}$, $70 \leq \mathrm{Re} \leq 1000$) at constant temperature ($T = 333$

K) under various pressure conditions: $CO_2$ pressure from 0 MPa to 15 MPa; transmembrane pressure between 0 and 0.8 MPa. Permeate samples were withdrawn after an approximately 1 h run with membrane T50C and weighed after total $CO_2$ elimination. Results are expressed as mass fluxes of pure PEG ($kg \cdot h^{-1} \cdot m^{-2}$) with an estimated precision of $\pm$ 1%.

As shown in Fig. 4, the addition of $CO_2$ under pressure improves permeate fluxes. However, this improvement remains limited, because under 15 MPa $CO_2$ pressure, the net flux increase reaches only 98% compared to the value obtained under atmospheric pressure.

Moreover, flux variation versus transmembrane pressure is not linear. This slower evolution may characterize fouling phenomena. Indeed, the hydrodynamic resistance associated with the membrane $R_m$, as calculated from the Darcy equation (Eq. 2) and measured viscosity data, increases with $CO_2$ or transmembrane pressures (Table 4).

$$J = \frac{\Delta P}{\mu R_m} = L_P \cdot \Delta P \tag{2}$$

where $J$ is the permeate flux, $\Delta P$ the transmembrane pressure, $\mu$ the viscosity of the solution, and $L_p$ the permeability of the membrane.

Another hypothesis that must be considered is the possibility of phase-separation phenomena at the entry of the pores, induced by the particular conditions in that region (e.g., high shear stresses, fouling), leading to a preferential passage of a $CO_2$-rich phase.

With low-pore-size membranes (T511 and T513), fluxes have been measured during the filtration of a $CO_2$-saturated mixture of PEG 400 and PEG

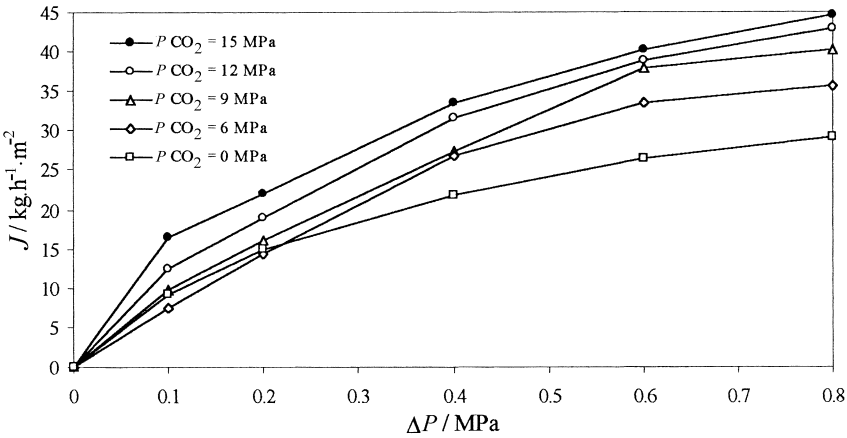


FIG. 4 Pure PEG 400 flux with membrane T50 C as a function of transmembrane pressure ($T$ = 333 K, $u \approx 0.7$ m·s$^{-1}$).

TABLE 4
Preliminary Filtration Experiments of $CO_2$-Saturated PEG 400 on the Coupling Bench Carried Associated to the Membrane

| | $P_{CO_2}$ = 6 MPa | | $P_{CO_2}$ = 9 MPa | |
|---|---|---|---|---|
| $\Delta P$/MPa | J/kg·hr$^{-1}$·m$^{-2}$ | $R_m$/m$^2$·kg$^{-1}$ | J/kg·hr$^{-1}$·m$^{-2}$ | $R_m$/m$^2$·kg$^{-1}$ |
| 0 | 0 | | 0 | |
| 0.1 | 7.54 | 5.54 $10^9$ | 9.84 | 5.77 $10^9$ |
| 0.2 | 14.45 | 5.78 $10^9$ | 16.06 | 7.07 $10^9$ |
| 0.4 | 26.77 | 6.24 $10^9$ | 27.41 | 8.29 $10^9$ |
| 0.6 | 33.57 | 7.46 $10^9$ | 37.93 | 8.98 $10^9$ |
| 0.8 | 35.70 | 9.36 $10^9$ | 40.16 | 11.31 $10^9$ |



1000 (25%–75% mass), and selectivities have been calculated through Eq. 3 (see Table 5).

$$\alpha_{1000}^{400} = \frac{C_{400}^{permeate}/C_{1000}^{permeate}}{C_{400}^{retentate}/C_{1000}^{retentate}} \quad (3)$$

Permeate fluxes obtained with the low-pore-size UF membranes (T511 and T513), for a given transmembrane pressure, are lower than fluxes recorded with the medium-pore-size element (T50C), as would be expected. The increase of $CO_2$ pressure allows a significant improvement in permeate flow rates. As an example, with membrane T511, under a 3 MPa transmembrane pressure, an increase of $CO_2$ pressure from 0 to 12 MPa increases the PEG mass flow rate from 5.27 hr$^{-1}$·m$^{-2}$ to 19.64 kg. hr$^{-1}$·m$^{-2}$ (i.e., 272%). On

TABLE 5
Flux and Selectivity of the Membranes T511 and T513 During the Filtration of $CO_2$-Saturated PEG 400-PEG 1000 Mixture on the Coupling Bench ($T$ = 333 $K$, $u \approx 0.7$ ms$^{-1}$)

| | T511 | | | | | | T513 | |
|---|---|---|---|---|---|---|---|---|
| | $P_{CO_2}$ = 0 MPa | | $P_{CO_2}$ = 6 MPa | | $P_{CO_2}$ = 12 MPa | | $P_{CO_2}$ = 12 MPa | |
| $\Delta P$/MPa | J/kg·hr$^{-1}$·m$^{-2}$ | $\alpha_{1000}^{400}$ | J/kg·hr$^{-1}$·m$^{-2}$ | $\alpha_{1000}^{400}$ | J/kg·hr$^{-1}$·m$^{-2}$ | $\alpha_{1000}^{400}$ | J/kg·hr$^{-1}$·m$^{-2}$ | $\alpha_{1000}^{400}$ |
| 0.5 | — | — | — | — | 12.40 | 1.03 | — | — |
| 1 | — | — | 6.20 | 1.22 | 14.47 | 1.04 | 2.17 | 1.24 |
| 2 | — | — | 8.27 | 1.20 | 17.57 | 1.11 | 3.07 | 1.36 |
| 3 | 5.27 | 1.23 | 10.34 | 1.21 | 19.64 | 1.06 | 3.61 | 1.49 |

Out with the Membrane T50 C ($T = 333$ K, $u \approx 0.7$ ms$^{-1}$); Calculated Values for the Resistance $R_m$ with Darcy Equation

| $P_{CO_2} = 12$ MPa | | $P_{CO_2} = 15$ MPa | |
|---|---|---|---|
| J/kg·hr$^{-1}$·m$^{-2}$ | $R_m$/m$^2$·kg$^{-1}$ | J/kg·hr$^{-1}$·m$^{-2}$ | $R_m$/m$^2$·kg$^{-1}$ |
| 0 | | 0 | |
| 12.41 | $5.70\ 10^9$ | 16.51 | $4.94\ 10^9$ |
| 18.91 | $7.48\ 10^9$ | 21.97 | $7.43\ 10^9$ |
| 31.60 | $8.95\ 10^9$ | 33.57 | $9.73\ 10^9$ |
| 38.89 | $10.91\ 10^9$ | 40.16 | $12.20\ 10^9$ |
| 42.92 | $13.18\ 10^9$ | 44.62 | $14.64\ 10^9$ |



the other hand, the resulting selectivity ($\alpha_{1000}^{400}$) is lower: from 1.23 to 1.06.

It appears that membrane T511 allows higher permeate fluxes than membrane T513, but with a lower selectivity. This fact can be explained by the existence of nonsimilar interactions between products and membrane materials. However, the difference in hydrodynamics between the systems seems to be of much greater effect. Indeed, the two membranes have different geometric characteristics and thus work under different hydrodynamic conditions ("clover" geometry for the membrane T511, and "monocanal" structure for the membrane T513). The mass-transfer-coefficient value, $k$, can be calculated for each module using the Chilton-Colburn analogy relation (18)

$$St_m \cdot Sc^{2/3} = \frac{\lambda}{8} \tag{4}$$

where $St_m$ and $Sc$ are the dimensionless Stanton and Schmidt numbers respectively, and $\lambda$ is the friction coefficient.

The Schmidt number is given by relation (5)

$$Sc = \frac{\mu}{\rho D_{AB}} \tag{5}$$

where $\mu$ and $\rho$ are the mean fluid viscosity and density, respectively, and $D_{AB}$ is the binary diffusion coefficient.

The Stanton number is given by relation (6):

$$St_m = \frac{k}{u} \tag{6}$$

where $u$ is the fluid velocity in the module.

The calculation of the $u$ and the Reynolds number ($Re$) as a function of the $CO_2$ pressure gives, for the two membranes

- at $P_{CO2} = 0$ MPa:

  T511: $u = 0.76\ m{\cdot}s^{-1}$ $\quad Re = 68$

  T513: $u = 0.65\ m{\cdot}s^{-1}$ $\quad Re = 113$

- at $P_{CO2} = 12$ MPa:

  T511: $u = 0.77\ m{\cdot}s^{-1}$ $\quad Re = 607$

  T513: $u = 0.66\ m{\cdot}s^{-1}$ $\quad Re = 1011$

In laminar flow conditions, the friction coefficient λ is given by

$$\lambda = \frac{64}{Re} \tag{7}$$

From (4) to (6) we therefore obtain the following expression for $k$

$$k = \frac{8}{d} \cdot \left(\frac{\mu}{\pi}\right)^{1/3} \cdot D_{AB}^{1/3} \tag{8}$$

As a result, the mass-transfer-coefficient ratio between the two membranes is given by

$$\frac{k_{T511}}{k_{T513}} = \frac{d_{T513}}{d_{T511}} \tag{9}$$

The calculation gives, in laminar flow, a ratio of approximately 1.9 resulting from the smaller channel diameter of membrane T511 ($3.6\ 10^{-3}$ m) versus membrane T513 ($7\ 10^{-3}$ m).

As seen in Eq. (8), mass-transfer coefficients in membrane systems are dependent on the viscosity and the density of the fluid ($k \propto (\mu/\rho)^{1/3}$), but they are also strongly dependent on the binary diffusion coefficients ($k \propto D^{2/3}{}_{AB}$). This is a particularly important effect in this system where the dissolution of $CO_2$ is expected to significantly improve the diffusivity of the polymer chains. Unfortunately, experimental data are scarce (19) for SC $CO_2$-saturated liquids, and it was not possible to estimate these values.

When a membrane rejects a solute, it accumulates on the membrane surface and creates a polarized layer that increases the resistance to permeation. This phenomenon, called "concentration polarization," is an unavoidable consequence of UF that can be attenuated by increasing the fluid shear rate, i.e., the fluid velocity. Under steady-state flow conditions, the permeate flux $J$ can be expressed by the following equation based on the film theory

$$J = k \ln\left(\frac{C_w - C_P}{C_b - C_P}\right) \tag{10}$$

where $C_w$, $C_b$, and $C_P$ are the wall concentration, the bulk concentration, and the permeate concentration, respectively.

The higher mass-transfer coefficient in the T511 membrane should reduce the extent of polarization (i.e., it should reduce the accumulation of rejected PEG at the membrane surface), which will in turn increase the permeate flux resulting from the reduction in osmotic pressure of the rejected PEG. Concentration polarization, and therefore hydrodynamics, will also affect the selectivity, because the larger PEG will polarize to a greater extent than the smaller PEG (because of its smaller diffusivity). As a result, the lower mass-transfer coefficient in the T513 module is responsible for higher selectivity (Table 5).

Moreover, the concentration-polarization phenomenon is also consistent with the reduction in selectivity with increasing the $CO_2$ pressure (Table 5). Indeed, the increase of $CO_2$ pressure will cause a greater increase in the concentration of the larger PEG at the membrane surface because of its smaller diffusivity. This will in turn cause a greater increase in transmission of the larger PEG, thereby reducing the selectivity.



### *FILEAS Bench*

The entire set of experiments was carried out with higher tangential fluid velocity and flow regime than with the coupling bench ($Q_m \approx 600$ kg·h$^{-1}$, $u \approx 5$ m·s$^{-1}$, $400 \leq Re \leq 5600$). Three temperatures, close to those corresponding to the solubility measurements, were selected: 313 K, 333 K, and 343 K. Medium-pore-size membranes (T50 A and T50 B) were tested.

Results obtained with PEG 400 at 333 K are represented in Fig. 5. Pure PEG mass fluxes and permeabilities were calculated from on-line measurements of

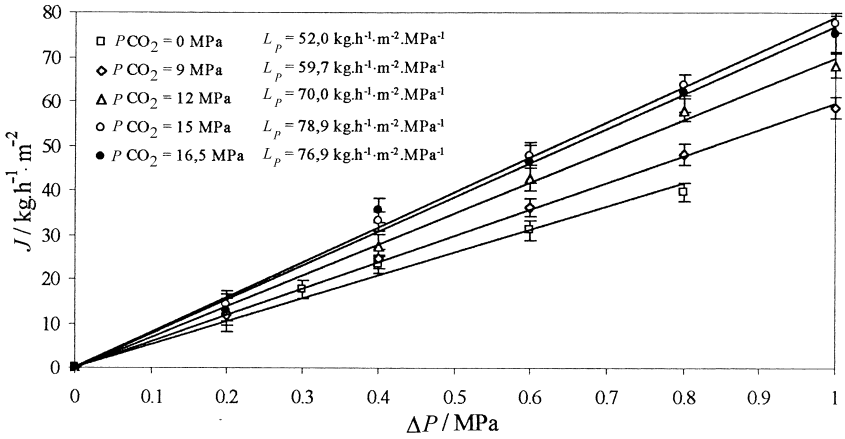


FIG. 5 Pure PEG 400 flux with membranes T50 A and T50 B (cutoff: 50 kDa), as a function of transmembrane pressure. Corresponding permeabilities. ($T = 333$ K, $u \approx 5$ m·s$^{-1}$).

TABLE 6
Permeability in PEG 400 Measured at 313 K, 333 K, and 343 K on the FILEAS Resistance Associated to the Membrane $R_m$ with

| | $T = 313$ K | |
|---|---|---|
| $P_{CO_2}$/MPa | $L_p^{PEG}$/kg·hr$^{-1}$·m$^{-2}$·MPa$^{-1}$ | $R_m$/m$^2$·kg$^{-1}$ |
| 0 | 31.9 | 2.52 $10^9$ |
| 9 | | |
| 10 | 48.6 | 11.40 $10^9$ |
| 12 | 51.7 | 11.80 $10^9$ |
| 15 | 54.8 | 11.94 $10^9$ |
| 16.5 | | |
| 18 | 57.7 | 11.55 $10^9$ |
| Maximum yield (%) | 81 | |



mass permeate throughout (PEG 400 + $CO_2$) and solubility values previously determined on the assumption of homogeneity of the mixture. Error intervals are indicated. Each measurement corresponds approximately to a 1 h filtration run.

With FILEAS there is a linear variation of pure PEG flux as a function of transmembrane pressure. Fouling and phase separation of the mixture at the membrane wall previously mentioned seems to have disappeared. The only working parameter whose variation from one bench to the other is high enough to explain such a fact is the tangential flow rate in the membrane (lower than 1 m·s$^{-1}$ with the coupling bench and approximately 5 m·s$^{-1}$ with the FILEAS bench). This result confirms that flux-limiting phenomena take place at the surface of the membrane rather than in the pores.

At 313 K the increase in permeability of pure PEG is all the more marked as the pressure of $CO_2$ is higher. However, for temperatures above 333 K, a maximum permeability is reached at $P_{CO2} = 15$ MPa. The use of a higher gas pressure is no longer justified because the positive effect of a complementary injection of $CO_2$ for a viscosity reduction is compensated for by an unfavorable effect of PEG dilution in the mixture that lowers the net PEG mass flux in the permeate.

The values of permeability and resistance associated to the membrane $R_m$ are shown in Table 6. The maximum gains in permeability are also indicated for each temperature. The evolution of $R_m$ as a function of the $CO_2$ pressure differs from that observed with the coupling bench; there is no significant influence of the $CO_2$ pressure on $R_m$ for pressure higher than 9 MPa. This is consistent with fouling phenomena that would occur preferentially at the membrane surface and that would not be observed with the FILEAS bench.

Bench with Membranes T50 A and T50 B ($u \approx 5$ m·s$^{-1}$); Calculated Values for the Darcy Equation; Corresponding Maximum Yields

| $T = 333$ K | | $T = 343$ K | |
|---|---|---|---|
| $L_p^{PEG}$/kg·hr$^{-1}$·m$^{-2}$·MPa$^{-1}$ | $R_m$/m$^2$·kg$^{-1}$ | $L_p^{PEG}$/kg·hr$^{-1}$·m$^{-2}$·MPa$^{-1}$ | $R_m$/m$^2$·kg$^{-1}$ |
| 52.0 | $3.23\ 10^9$ | 94.3 | $2.29\ 10^9$ |
| 59.7 | $9.57\ 10^9$ | | |
| 70.0 | $10.08\ 10^9$ | 124.1 | $6.17\ 10^9$ |
| 78.9 | $10.37\ 10^9$ | 127.9 | $6.86\ 10^9$ |
| 76.9 | $11.15\ 10^9$ | | |
| | | 122.6 | $7.94\ 10^9$ |
| 52 | | 36 | |



As a whole, looking at the maximum permeability gain values obtained by adding $CO_2$, it appears that increasing the temperature has an unfavorable influence on filtration performance. A similar conclusion has already been made in the laboratory viscosity measurements.

## CONCLUSION

This study presents a new process for the filtration of highly viscous liquids at low temperatures. The principle of this process is to lower the fluid viscosity by injecting pressurized $CO_2$ before filtration. This initial study was conducted using model compounds, polyethylene glycols (PEG). First, the physicochemical characteristics of PEG in the presence of $CO_2$ (mainly viscosity and phase-equilibrium data) were measured at various pressure and temperature conditions. Then, filtration of various PEG-$CO_2$ mixtures with two different pilot-plant units validated the process.

The dissolution of a small quantity of $CO_2$ leads to a significant viscosity reduction. The most significant effect (89%) was reached with PEG 400 at 313 K and 25 MPa (final viscosity value approximately 5 mPa·s). The corresponding amount of $CO_2$ dissolved in the mixture was approximately 30% (by mass).

As a whole, filtration experiments conducted with PEG on ceramic membranes indicate that by decreasing viscosity the addition of pressurized $CO_2$ enables a net improvement of PEG mass flux through the membrane. However, the evolution of the permeate flux as a function of transmembrane pressure is linear on the FILEAS bench, whereas it is slower on the coupling bench. The difference thus observed seems to be related to the use of a higher

tangential fluid velocity in the first case, which probably prevents limitations at the wall: superficial fouling resulting from PEG deposition, phase separation because of high shear stresses, and preferential passage of $CO_2$. Finally, an optimum working pressure was obtained on the FILEAS bench when the temperature was increased; for this value the opposite effects that result from a lower viscosity and an increased dilution of PEG counterbalance each other.

## NOMENCLATURE

| | |
|---|---|
| $C$ | concentration ($g \cdot dm^{-3}$) |
| $d$ | diameter (m) |
| $D_{AB}$ | binary diffusion coefficient ($m^2 \cdot s^{-1}$). |
| $J$ | flux ($kg \cdot hr^{-1} \cdot m^{-2}$) |
| $k$ | mass-transfer coefficient ($m \cdot s^{-1}$) |
| $L_p$ | permeability ($kg \cdot hr^{-1} \cdot m^{-2} \cdot bar^{-1}$) |
| $P$ | pressure (MPa) |
| PEG | Polyethyleneglycol |
| $Q_m$ | mass flow rate ($kg \cdot hr^{-1}$) |
| $r$ | number of lattice sites occupied by a molecule |
| $Re$ | Reynolds number |
| $R_m$ | resistance associated to the membrane ($m^2 \cdot kg^{-1}$) |
| $Sc$ | Schmidt number |
| $St_m$ | Stanton number |
| $T$ | temperature (K) |
| $u$ | average axial velocity ($m \cdot s^{-1}$) |
| $\alpha$ | selectivity factor |
| $\lambda$ | friction coefficient |
| $\mu$ | viscosity (Pa·s) |
| $\rho$ | density ($kg \cdot m^{-3}$) |

### Superscript

| | |
|---|---|
| ~ | reduced parameters |

### Subscripts

| | |
|---|---|
| $b$ | bulk |
| $p$ | permeate |
| $w$ | wall |

## REFERENCES

1. P. Brassart, "Used Oil Management Regulations: A Comparison of the European Economic Community with the United States," *Second International Congress on Liquid Waste Recycling*, Las Vegas, Nev., June 12–14, 1996.

2. J. Arod, B. Bartoli, P. Bergez, J. M. Biedermann, P. Caminade, J. M. Martinet, J. Maurin, and J. Rossarie, *High-Temperature Ultrafiltration Treatment of a Hydrocarbon Load*, Patent EP 400793, 1981.
3. P. D'amore and S. Mirmiran, *Microfiltration of Used Oil*, Patent WO 95/08609, 1995.
4. A. Duong, G. Chattopadhyaya, W. Y. Kwok, and K. J. Smith, "An Experimental Study of Heavy Oil Ultrafiltration Using Ceramic Membranes," *Fuel, 76*(9), 821 (1997).
5. D. Defives, R. Avrillon, C. Miniscloux, R. Roullet, and X. Marze, "Regeneration of Used Lubricating Oils by Ultrafiltration," *Inf. Chimie, 175*, 127 (1978).
6. G. Hotier, *Procédé de désasphaltage d'une huile d'hydrocarbure renfermant de l'asphalte*, Patent FR 2,598,717, 1987.
7. E. Hartmann and A. G. Bucher-Guyer, *Cross-Flow Filtering Process for Separating Fluid from a Free-Flowing Medium and Installation for Implementing It*, Patent WO 96/36426, 1996.
8. K. Chin, C. Crabb, G. Ondrey, and T. Kamiya, "Supercritical Fluids Stay Solvent," *Chem. Eng., 32*, Oct. (1998).
9. R. Noyori, "Supercritical Fluids," *Chem. Rev., 99*(2), 353 (1999).
10. S. Sarrade, G. M. Rios, and M. Carles, "Supercritical $CO_2$ Extraction Coupled with Nanofiltration Separation. Application to Natural Products," *Sep. Purif. Technol., 14*, 19 (1998).
11. M. McHugh and V. Krukonis, *Supercritical Fluid Extraction*, 2d ed., Butterworth-Heinemann, Boston, 1994.
12. Y. C. Bae, *Viscosity reduction of polymeric liquids by dissolved gases*, Ph.D. Thesis, Wayne State University, Detroit, 1989.
13. D. Gourgouillon, H. M. N. T. Avelino, J. M. N. A. Fareleira, and M. Nunes da Ponte, "Simultaneous Viscosity and Density Measurement of Supercritical $CO_2$-Saturated PEG 400," *J. Supercrit. Fluids, 13*, 177 (1998).
14. L. Schrive, D. Gourgouillon, M. Nunes da Ponte, G. M. Rios, and S. Sarrade, "Ultrafiltration Applied to Viscous Liquids Fluidified with Supercritical Carbon Dioxide, *Proceedings of the Fifth International Conference on Inorganic Membranes*, June 22–26, Nagoya, Japan, 298–301, 1998.
15. D. Gourgouillon and M. Nunes da Ponte, "High-Pressure Phase Equilibrium for Poly(Ethyleneglycol)s + $CO_2$: Experimental Results and Modelling," *Phys. Chem. Chem. Phys., 1*(23), 5369–5376 (1999).
16. J. A. Lopes, D. Gourgouillon, P. J. Pereira, A. M. Ramos, and M. Nunes da Ponte, "On the Effect of Polymer Fractionation on Phase Equilibrium in $CO_2$+Poly(ethylene glycol)s Systems," *J. Supercrit. Fluids, 16*(3), 261 (2000).
17. R. H. Lacombe and I. C. Sanchez, Statistical Thermodynamics of Fluid Mixtures, *J. Phys. Chem., 80*(23), 2568 (1976).
18. R. H. Perry and D. W. Green (Eds.), *Chemical Engineers' Handbook*, 7th Ed., Chap. 5, McGraw-Hill, New York, 1997, p. 79.
19. G. Brunner, *Gas Extraction* (H. Baumgartel, E. U. Franck, and W. Grunbein, Eds.), Springer, New York, 1994, p. 51.

*Received by editor October 11, 1999*
*Revision received February 2000*